# Electronic structure of Zn and Be doped GaAs photocathodes: a first-principles research

XIAOHUA YU*, GUIRONG SHAO, HUIXIA SUN
*Department of Physics and Electronic Engineering, Yuncheng University, Yuncheng 044000, China*

Based on the first-principle plane wave pseudopotential method, the bonding structure, E-Mulliken population, band structure and density of state (DOS) of Zn and Be substituted and interstitial doping GaAs models were calculated. Result showed that substitution doped GaAs materials were easier to form, they showed p-type characteristic and were suitable for the preparation of photocathodes. The Zn substitution doped GaAs showed better p-type property. Interstitially doping introduced mid-gap state and exhibited n-type characteristics. The change of the DOS in the Zn-Sub model was more obvious than that in the Be-Sub model. The change of DOS in Be-Inter model is more obvious than that in Zn-Inter model.

(Received July 9, 2019; accepted April 9, 2020)

*Keywords:* Semiconductors, Doping, Electronic structure, First-principles

## 1. Introduction

With excellent photoemission performance, such as: high spectral response sensitivity, low dark current, high spin polarization, high current density and concentrated emission energy and angular distribution. Negative Electron Affinity (NEA) GaAs photocathodes have been widely used in weak light detection field and in high-energy physics field, such as: electron beam planar exposure, linear accelerator and the first four-generation light sources [1-4].

GaAs photocathodes are usually prepared by cesium oxygen activation on high p-type doped GaAs surface [5,6] in ultra-high vacuum system. P-type GaAs substrates grown by molecular beam epitaxy (MBE) and metal organic chemical vapor deposition (MOCVD) are usually doped by Be or Zn atoms. Some researcher speculated that Zn was better doping elemen [7], they explanation is that "Since Be atom was smaller than Zn atom, after doping Be atoms are trend to form interstitial doping while Zn atoms are trend to form substituted doping." However, there was still no systemically theoretical research on doping element and doping method of GaAs. In the present article, substituted and interstitial doping GaAs models with Zn and Be atoms were built, through first-principles quantum mechanics method [8,9], the bonding structure, E-Mulliken population, band structure and density of state (DOS) of intrinsic and doped GaAs were calculated, the influence of doping atoms on electronic structure of GaAs substrate were analyzed.

## 2. Calculated method and models

The calculations were performed through the quantum mechanics program Cambridge Serial Total Energy Package (CASTEP) [10]. The exchange and correlation interactions in the calculation were treated by generalized gradient approximation (GGA) with the Perdew-Burke-Ernzerhof functional [11,12]. The ultrasoft pseudopotential [13], which were generated from Ga:$3d^{10}4s^24p^1$, As:$4s^24p^3$, Zn Zn:$3d^{10}4s^2$ and Be $2s^2$, were employed to describe the interaction between the ionic core and valence electrons. The calculated GaAs model was zinc-blende 2×2×2 supercell, which was consist of 32 Ga atoms and 32 As atoms. Four doping models were respectively built by substituting one Ga atom with one Zn atom (indicated as Zn-Sub), substituting one Ga atom with one Be atom (indicated as Be-Sub), inserting one Zn atom in GaAs model (indicated as Zn-Inter) and inserting one Be atom in GaAs model (indicated as Be-Inter). The Broyden- Fletcher-Goldfarb-Shanno (BFGS) algorithm was used to relax the structure of the crystal model. The calculation was taken with an energy cutoff of 330eV. The convergence precision were set as following: energy change below $2\times10^{-6}$eV/atom, force less than 0.001eV/nm, the convergence tolerance of a single atomic energy below $5\times10^{-6}$eV/atom. The integral in the Brillouin [14] zone was sampled with the Monkhorst-Pack [15] scheme and the number of k points was 7×7×7.

## 3. Results and discussion

The lattice constants of GaAs after optimization was a=b=c=0.565315nm, which was in good agreement with

the experimental value [16], showing the correctness of the calculation method. Cohesive energy [17] (the energy needed to separate the material into free atoms) was used to analyze the stability of the doping models. The cohesive energy of intrinsic GaAs model, Zn-Sub model, Be-Sub model, Zn-Inter model and Be-Inter model were relatively -4.561eV, -4.485eV, -4.550eV, 27.111eV and 27.045eV. After doping the stability were lowered, Zn-Sub and Be-Sub models were still stable while Zn-Inter and Be-Inter models were unstable. The results showed that it was easier to form substituted doping materials during GaAs substrate growth. The influence of Zn atom on stability was more obvious than Be atom. This was attributed to that the covalent radius of Zn and Be was 0.09 nm and 0.125 nm respectively, therefore Be was easier to form doped materials than Zn.

### 3.1. E-Mulliken population

The bond population result can represent the property of a bond, a plus value means that the bond is a covalent bond while the minus value means a ionic bond. The larger absolute value of bond population shows stronger covalence or ionicity. The bond structure and E-Mulliken population of intrinsic GaAs, Zn-Sub and Be-Sub models were concluded in Table 1. In the intrinsic GaAs model, Ga loss 0.22electron per atom while As got 0.22 electron per atom, forming polar covalent Ga-As bonds. In Zn-Sub and Be-Sub models, Zn and Be got electron, at the same time As got less electrons while Ga loss less electrons.

The influence of Be on electron redistribution is more obvious. Bond calculation results showed that Zn-As bonds were longer than Ga-As bonds while Be-As bonds were shorter than Ga-As bond. The covalence of Zn-As bond was stronger than Ga-As bond while the covalence of Be-As bond was weaker than Ga-As bond. After substituted doping the covalence of Ga-As bonds were enhanced and the influence of Be was more obvious.

The bond structure and E-Mulliken population of intrinsic GaAs, Zn-Inter and Be-Inter models were concluded in Table 2. In Zn-Inter model, Zn loss electron, Ga loss less electron while As got more electron. In Be-Inter model, Be got electron, Ga loss less electron while As got more electron. The influence of Zn on electron redistribution was more obvious than Be. The length of Ga-As bonds near doping Zn and Be were lengthened while the covalence of these bonds were weakened. The lattice distortion and covalence change of Zn-Inter model was more obvious than Be-Inter model, this could be attributed to that the radius of Be was smaller than Zn. Results showed that Be-As bond and Be-Ga bond were shorter than Zn-As bond and Zn-Ga bond. Zn-As bonds were electrovalent bonds while Zn-Ga, Be-Ga and Be-As bonds were covalent bonds.

### 3.2. Band structure

The calculated band structures of intrinsic GaAs, Zn-Sub, Be-Sub, Zn-Inter and Be-Inter models were shown in Fig. 1. The band gap of intrinsic GaAs was 0.497eV, which was lower than the experimental value 1.424eV [18], this was a common phenomenon since the band gap was excited state, while the DFT calculation process is the ground state, but this did not affect the analysis of the electronic structure [19].

*Table 1. E-Mulliken population of GaAs Zn-Sub and Be-Sub models*

| | Ga-As bond | | Zn/Be-As bond | | Charge(\|e\|) | | |
|---|---|---|---|---|---|---|---|
| | length(Å) | population | length(Å) | population | Ga | As | Be/Zn |
| GaAs | 2.437 | 2.470 | -- | -- | 0.220 | -0.220 | -- |
| Zn-Sub | 2.435 | 2.618 | 2.477 | 2.723 | 0.203 | -0.208 | -0.070 |
| Be-Sub | 2.453 | 2.786 | 2.230 | 0.773 | 0.210 | -0.125 | -0.310 |

*Table 2. E-Mulliken population of GaAs Zn-Inter and Be-Inter models*

| | Ga-As bond | | Zn/Be-As bond | | Zn/Be -Ga bond | | Charge(\|e\|) | | |
|---|---|---|---|---|---|---|---|---|---|
| | length(Å) | population | length(Å) | population | length(Å) | population | Ga | As | Zn/Be |
| GaAs | 2.437 | 2.470 | -- | -- | -- | -- | 0.220 | -0.220 | -- |
| Zn-Inter | 2.489 | 2.200 | 2.890 | -0.603 | 2.552 | 1.058 | 0.138 | -0.242 | 0.110 |
| Be-Inter | 2.461 | 1.244 | 2.797 | 0.248 | 2.509 | 0.497 | 0.217 | -0.242 | -0.270 |

After doping, the valence bands of the Zn-Sub and Be-Sub model moved upwards, and the Fermi energy level entered the valence band, leading to p-type characteristic. The valence band maximum (VBM) of Zn-Sub moved upwards by 0.113eV while that of Be-Sub moved upwards by 0.112eV. Since the valence band movement of Zn-Sub model was larger, the p-type characteristic is better and Zn was more suitable as substituted doping element. The band gap of Zn-Sub and Be-Sub were respectively 0.472eV and 0.531eV, the band gap of Zn-sub was narrowed after doping and that of Be-Sub was widened.

The mid-gap states, introduced by interstitial doping, in Zn-Inter and Be-Inter models were located at 0.215eV and 0.231eV respectively. After interstitial doping the CBM and VBM moved downwards and the models showed n-type characteristic. CBM and VBM of Zn-Inter were located at 0.484eV and -0.091eV respectively while that in Be-Inter were located at 0.215eV and -0.242eV respectively. The influence of Be on band structure was more obvious and n-type characteristic of Be-inter model was more obvious.

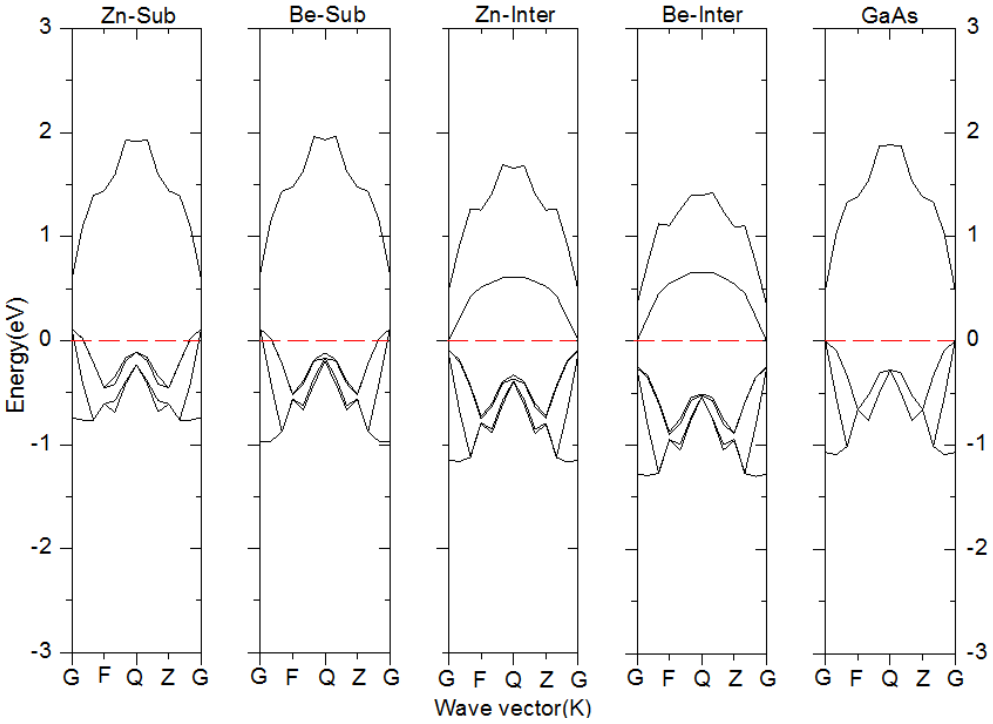


*Fig. 1. Band structure of intrinsic GaAs, Zn-Sub, Be-Sub, Zn-Inter and Be-Inter models*

### 3.3. DOS

The calculated DOS curves of intrinsic GaAs, Zn-Sub, Be-Sub, Zn-Inter and Be-Inter models were shown in Fig. 2. The pure GaAs had a deep energy level at -14.6eV, the valence band was composed of the upper valence band (located at -12.7~-9.5eV) and the lower valence band (located at -6.97~0eV). Lower valence band was mainly contributed by As-p state, upper valence band was mainly contributed by As-s, Ga-p and Ga-s states, the VBM was determined by As-p state. Conduction band was consist of As-s, As-p, Ga-s and Ga-p states. CBM was determined by the Ga-p state.

In the the doping models, the deep level at -14.6eV moved to the low energy side and the movements of interstitially doped models were more obvious. The movement of deep energy level in Be-Inter model was more obvious than that of Zn-Inter model while the movement of deep energy level in Zn-Sub model was more obvious than that of Be-Sub.

The CBM and VBM of Zn-Sub, Be-Sub, Zn-Inter and Be-Inter models are translated and the doping did not result in the redistribution of electrons. The distribution range of DOS peak were enlarged, the peak value were lowered, showing that the localization was weakened. The doping results in the enhancement of the interaction between atoms.

In Zn-Sub and Be-Sub, the Ga-s state at CBM increased the Ga-p state was invariance, and at VBM the Ga-s state was invariant as well as the Ga-p state at VBM. In Zn-Inter, Be-Inter models, the mid-gap states were contributed by Zn(Be)-s,Ga-s, Ga-p, Ga-s, As-s and As-p states commonly. In Zn-Inter model the contribution of Ga-s, Ga-p, As-s and As-p states to the mid-gap state was

more obvious than that in Be-Inter model. The interaction between doping atom and GaAs in Zn-Inter is more obvious. This was because that the ionicity of the Zn was more stronger that Be. In the CBM, Ga-s state was increased, Ga-p and As-p states were unchanged. In Zn-Sub model, As-s state was significantly increased, while the other states were slightly reduced. The interaction of Zn-As was more obvious. At VBM, the Ga-s, Ga-p and As-p states remained unchanged.

The concentration of conduction band electrons can be calculated by following formula:

$$n_0 = \frac{1}{V}\int_{E_C}^{\infty} f(E)g_c(E)dE \tag{1}$$

where, $g_c(E)$ is the density of state near conduction band bottom, $V$ is super-cell volume. The doping concentration in the calculation is 3.125%, belong to high-concentration doping, the models are belong to degenerate semiconductor, the electrons obey Fermi-Dirac distribution:

$$f(E) = \frac{1}{1+\exp(\frac{E_i - E_F}{k_B T})} \tag{2}$$

where $k_B$ is boltzmann's constant. The calculated carrier concentration of Zn-Sub and Be-Sub were respectively $1.223\times10^{22}$ $cm^{-3}$ and $1.221\times10^{22}$ $cm^{-3}$, the results showed that the Zn was better p-type doping element than Be.

## 4. Conclusion

Based on the first-principle plane-wave pseudopotential method, the bonding structure, E-Mulliken population, band structure and DOS of intrinsic GaAs, Zn-Sub, Be-Sub, Zn-Inter and Be-Inter models were calculated. The results showed that the stability was weakened after doping, and that it was easier to form substituted doping materials during GaAs substrate growth. The influence of Zn atom on stability was more obvious than Be atom. After substituted doping the covalence of Ga-As bonds were enhanced and the influence of Be was more obvious. The lattice distortion and covalence change of Zn-Inter model was more obvious than Be-Inter model. The valence bands of the Zn-Sub and Be-Sub models moved upwards, and the Fermi energy level entered the valence band, leading to p-type characteristic. Zn was more suitable as substituted doping element. Zn-Inter, Be-Inter models showed n-type characteristic. N-type characteristic of Be-Inter model was more obvious. Carrier concentration of Zn-Sub and Be-Sub were respectively $1.223\times10^{22}$ $cm^{-3}$ and $1.221\times10^{22}$ $cm^{-3}$, the results showed that the Zn was better p-type doping element than Be.

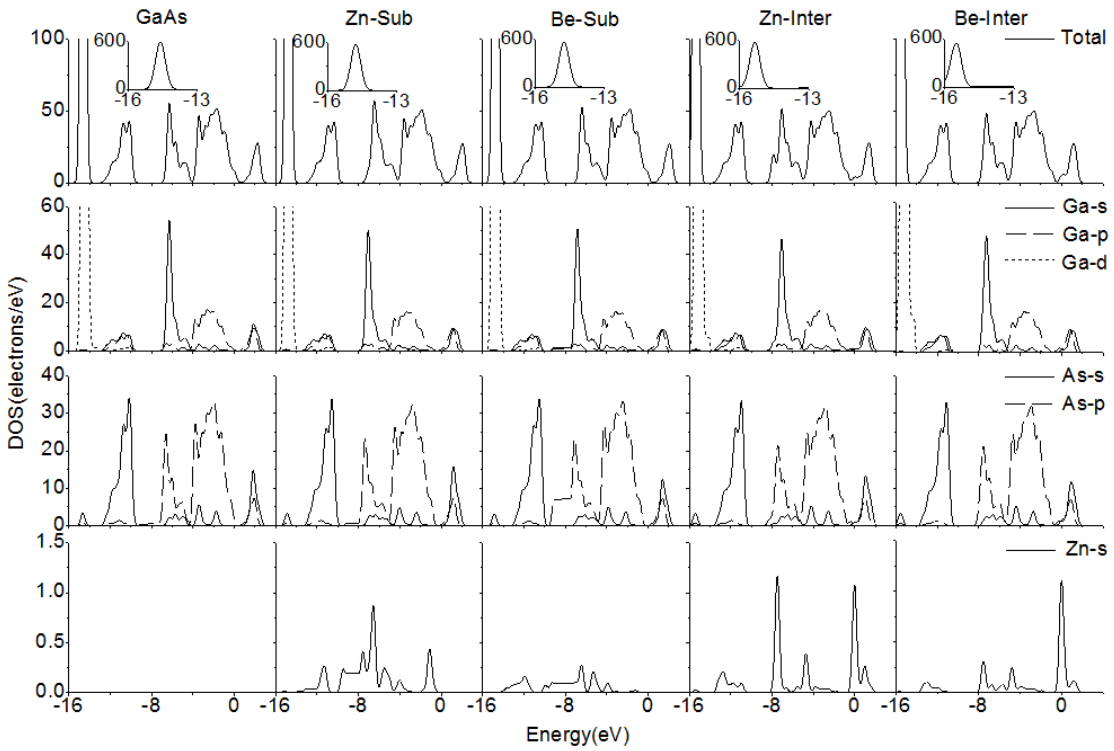


*Fig. 2. DOS curves of intrinsic GaAs, Zn-Sub, Be-Sub, Zn-Inter and Be-Inter models*

**Acknowledgement**

The authors would like to thank School of Information and Electrical Engineering, Ludong University for first-principles calculations. This work has been financially supported by the Natural Science Foundation of HuBei Province (Grant No. 2017CFB332).

## References

[1] Z. Liu, Y. Sun, S. Peterson, P. Pianetta, Appl. Phys. Lett. **92**, 241107 (2008).
[2] J. J. Zou, B. K. Chang, H. L. Chen, L. Liu, J. Appl. Phys. **10**, 1033126 (2007).
[3] F. Machuca, Z. Liu, Y. Sun, P. Pianetta, W. E. Spicer, R. F. W. Pease, J. Vac. Sci. Technol. B **21**,1863 (2003).
[4] T. Rao, A. Burrill, X. Y. Chang, J. Smedley, T. Nishitani, C. Hernandez Garcia, M. Poelker, E. Seddon, F. E. Hannon, C. K. Sinclair, J. Lewellen, D. Feldmang, Nucl. Instrum. Methods Phys. Res. A **557**, 124 (2006).
[5] V. L. Alperovich, A. G. Paulish, H. E. Scheibler, A.S. Terekhov, Appl. Phys. Lett. **66**, 2122 (1995).
[6] D. A. Orlov, M. Hoppe, U. Weigel, D. Schwalm, A.S. Terekhov, A. Wolf, Appl. Phys. Lett. **78**, 2721 (2001).
[7] X. L. Chen, Y. J. Zhang, B. K. Chang, P. Gao, J. Zhao, F. Shi, Optoelectron. Adv. Mat. **6**(1-2), 307 (2012).
[8] Q. Luo, G. Li, J. Xiao, C. Yin, Y. He, M. Wang, C. Ma, C. Zhu, J. Xu, J. Theor. Comp. Chem. **17**, 1850050 (2018).
[9] B. G. Kim, H. Sim, J. Park, Solid State Commun. **169**, 50 (2013).
[10] Y. J. Du, B. K. Chang, J. J. Zhang, B. Li, X. H. Wang, Acta Phys. Sin. **61**, 067101 (2012).
[11] W. Wang, K. Xiong, R. M. Wallace, K. Cho, J. Appl. Phys. **110**, 103714 (2011).
[12] D. M. Ceperley, B. J. Alder, Phys. Rev. Lett. **45**, 566 (1980).
[13] A. M. Silva, B. P. Silva, F. A. M. Sales, Phys. Rev. B **86**, 195201 (2012).
[14] J. P. Perdew, K. Burke, M. Ernzerhof. Appl. Phys. Lett. **77**, 3865 (1996).
[15] H. J. Monkhors, J. D. Pack, Phys. Rev. B **13**, 5188 (1976).
[16] http://www.ioffe.ru/SVA/NSM/Semicond/GaAs /basic.html
[17] S. Ulrich, A. Zippelius, Phys. Review Lett. 109, 166001 (2012).
[18] http://www.ioffe.ru/SVA/NSM/Semicond/GaAs /bandstr.html.
[19] W. E. Pickett, Comput. Phys. Rep. **9**, 115 (1989).

*Corresponding author: 624554818@qq.com